ACIM
HUP La Fe

Deep learning NMR and outcomes prediction

Leonor Cerdá Alberich

La Fe Health Research Institute (Valencia)

16.06.2022

Deep learning NMR

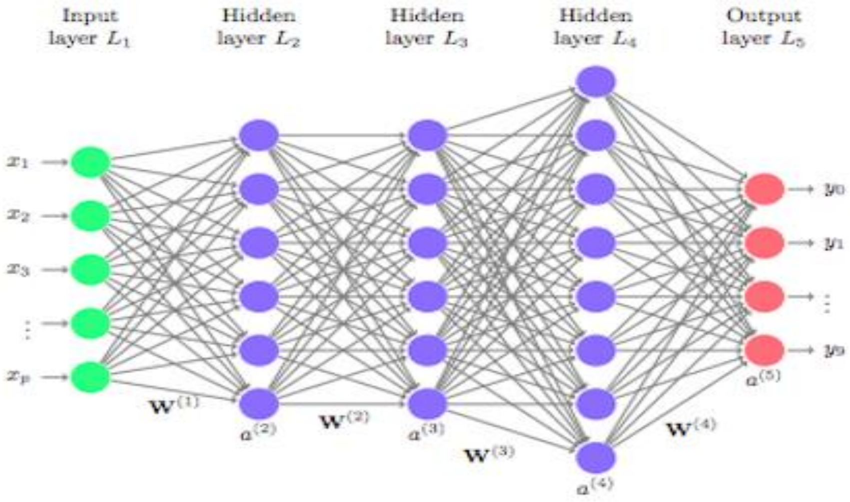

- **Input:** MR images
- **Output 1:** Tumor segmentation
- **Output 2:** Hallmarks
- **Output 3:** Diagnosis - Prediction
- **Output 4:** Decision on treatment

T2W

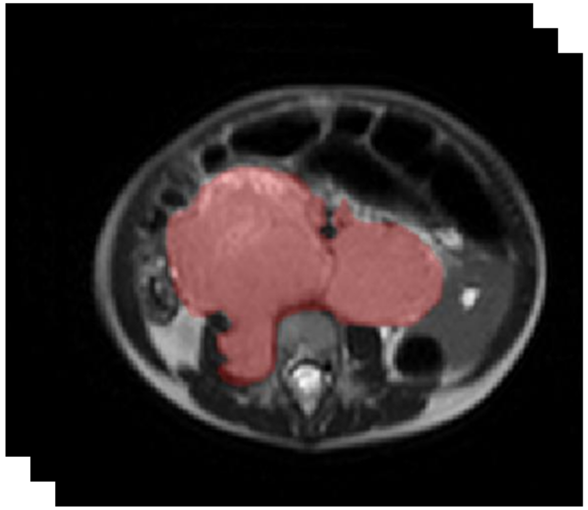

T1W

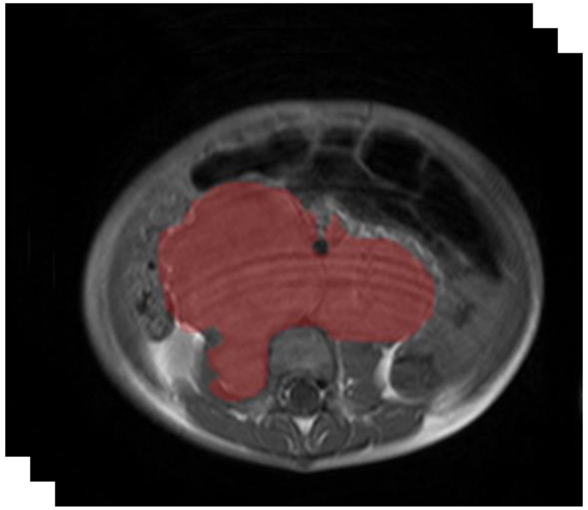

DWI

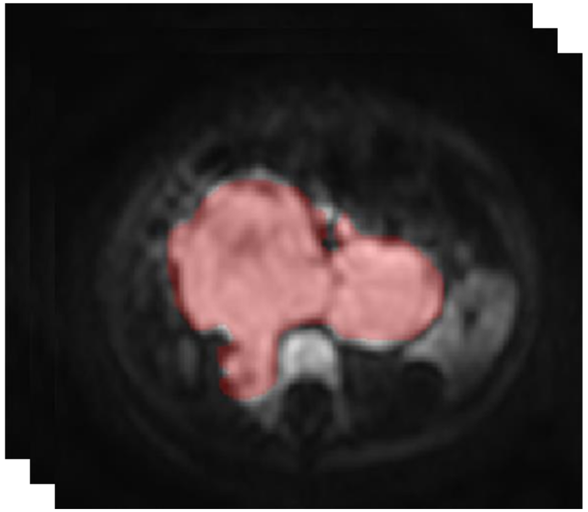

Virtual Biopsy in Oncology

ACIM
HUP La Fe

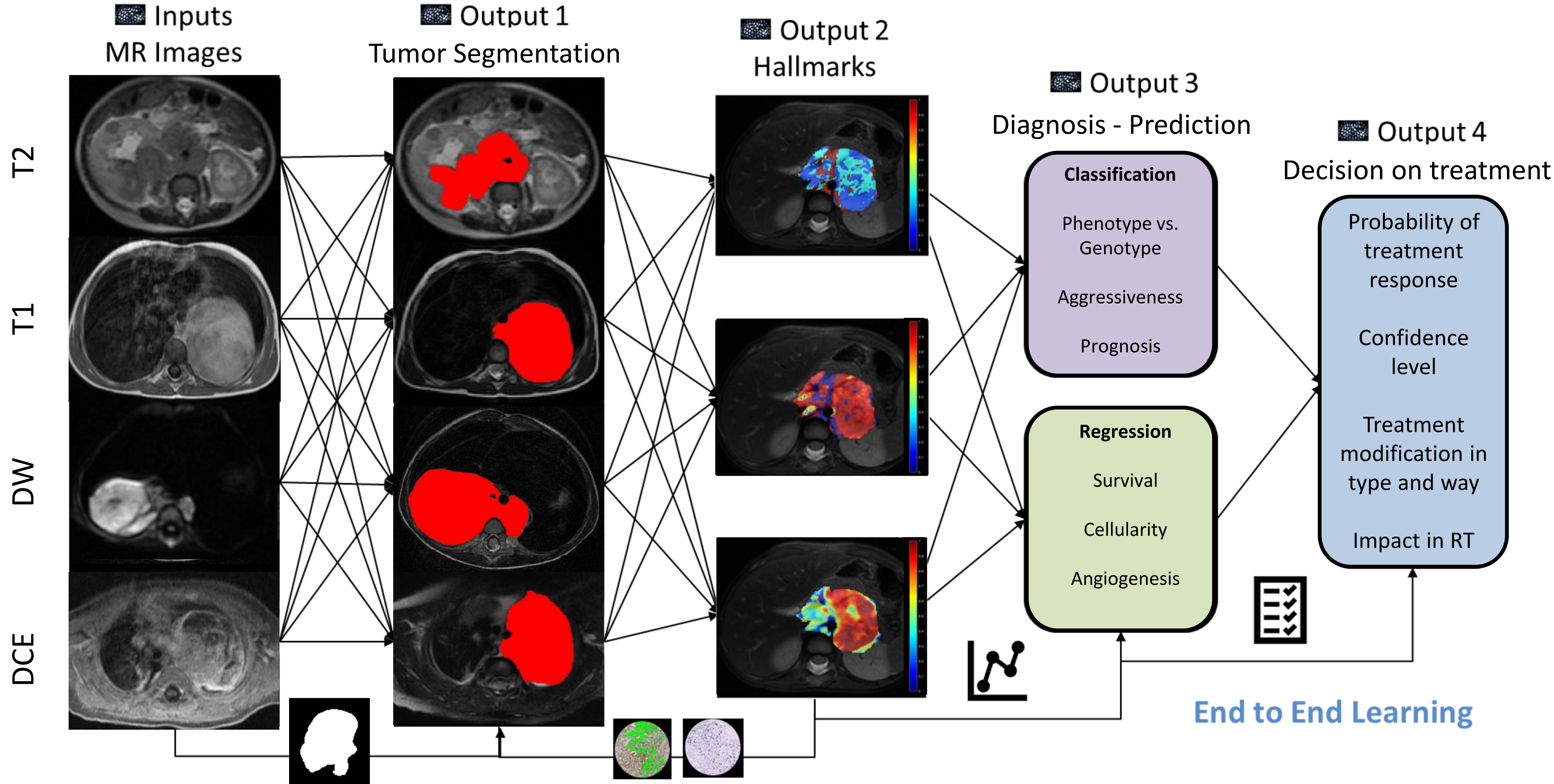

GIBI2 30
GRUPO DE INVESTIGACIÓN BIOMÉDICA EN IMAGEN

ACIM
HUP La Fe

Image processing pipeline

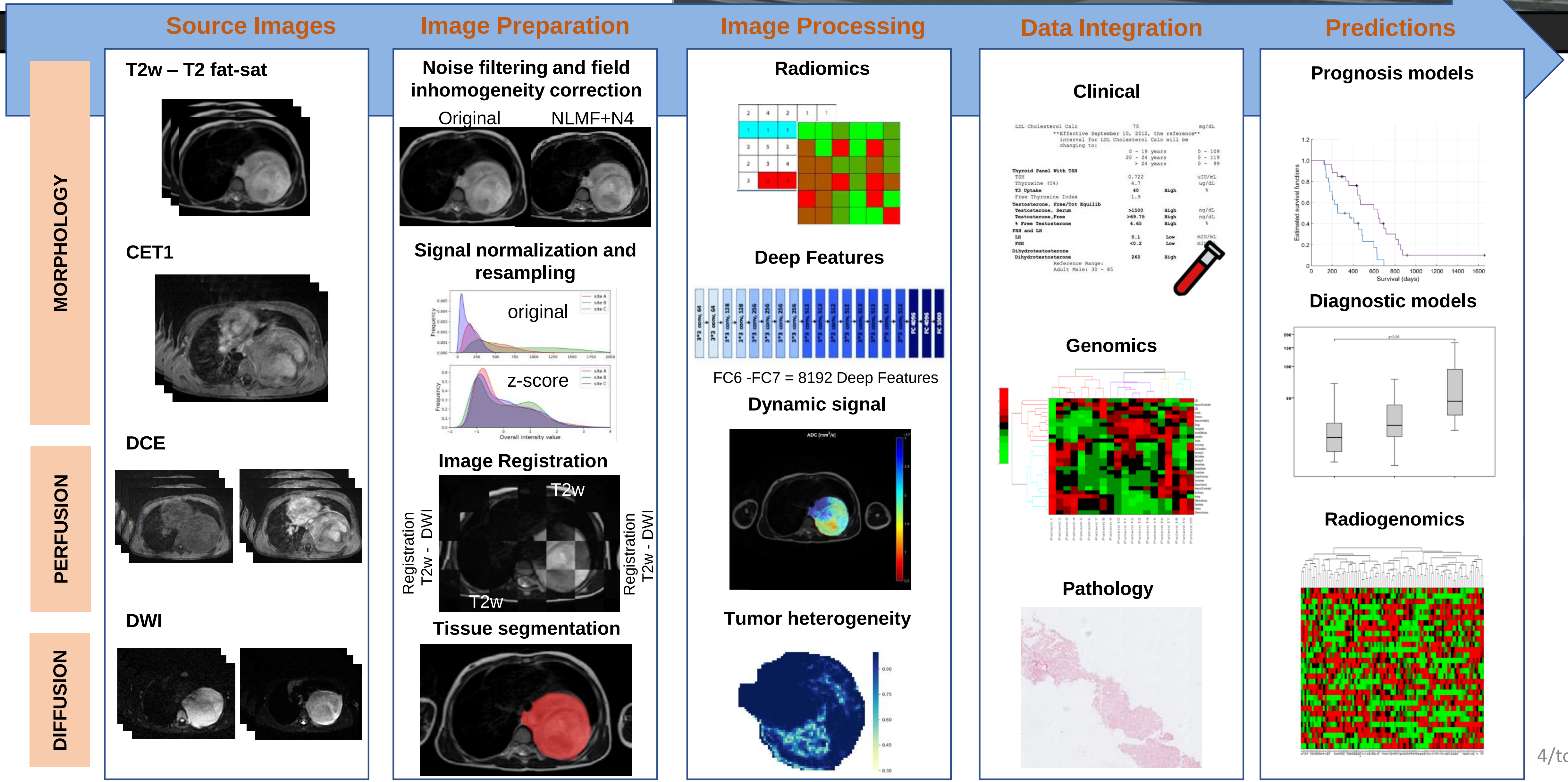

ACIM HUP La Fe

Image harmonization

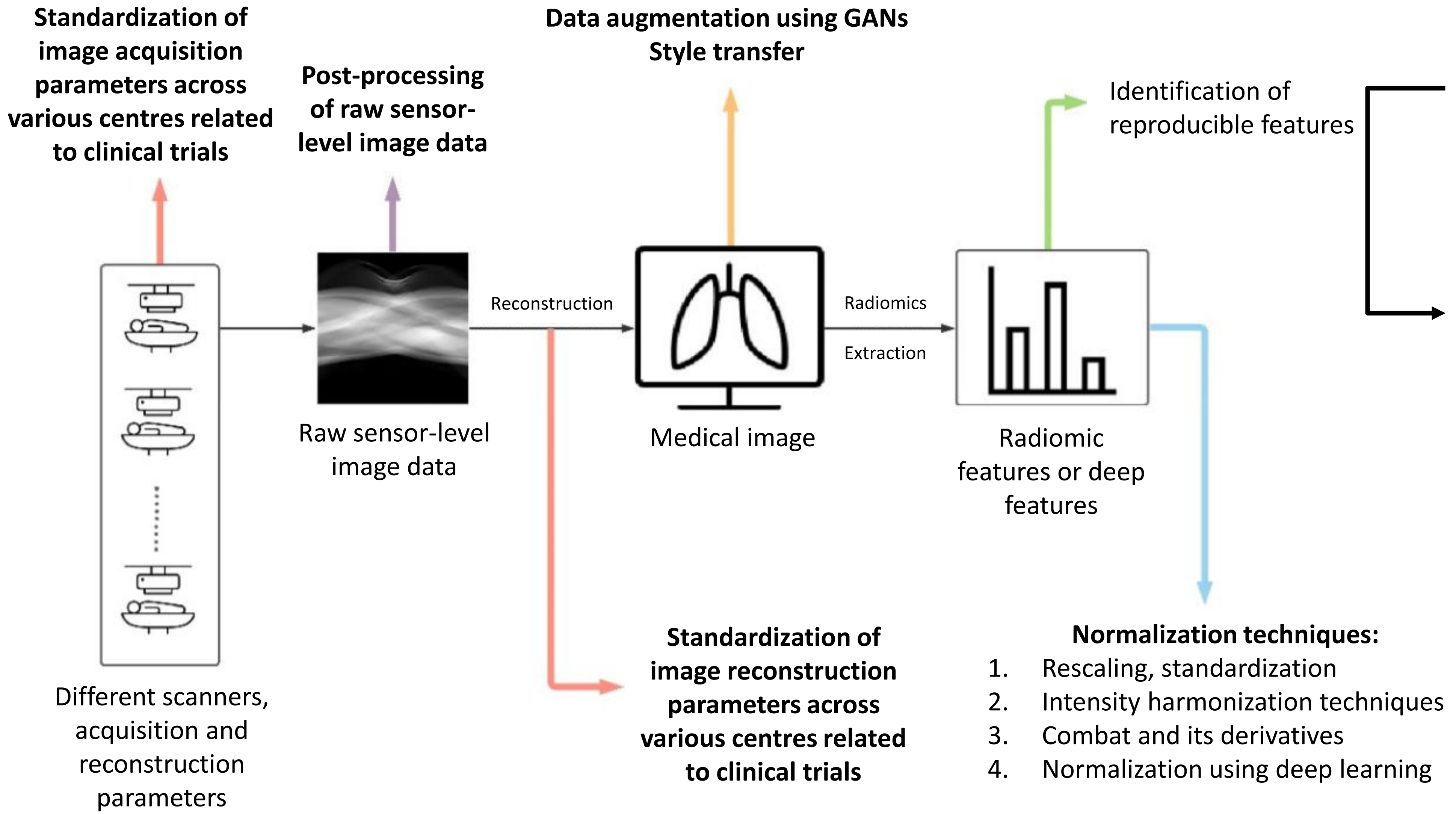

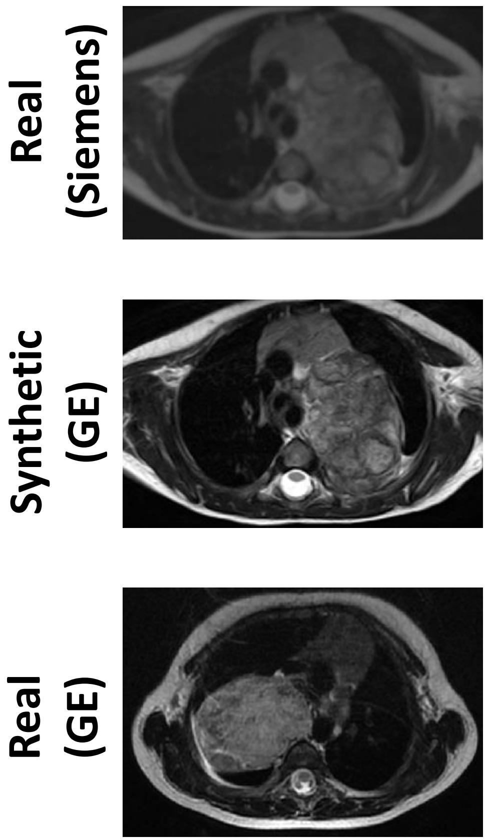

Image Synthesis

ACIM

HUP La Fe

Generative adversarial networks (GAN)

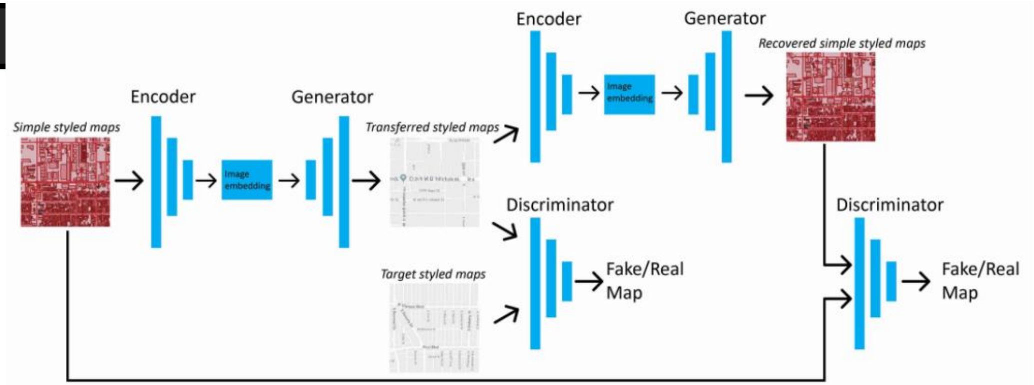

The images were harmonised by the **CycleGAN**-based module to achieve a better resolution and low noises

Visualization results of Cycle-GAN for **MRI image harmonization**

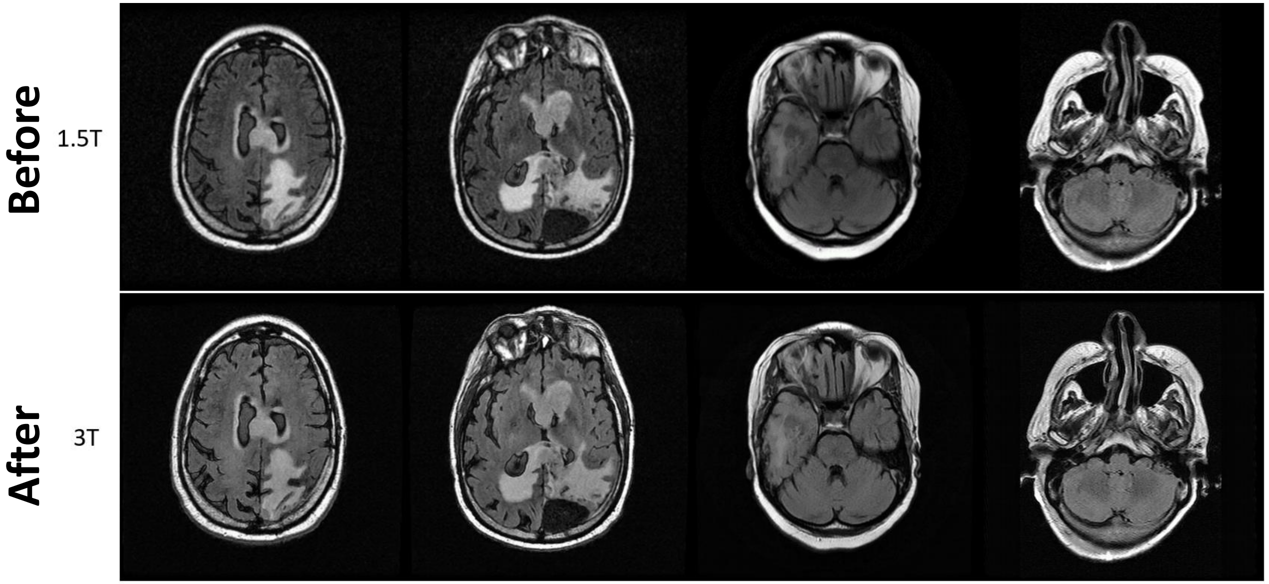

Effect of image harmonization on computational models

A simple ResNet50 classifier is trained on the TCGA brain tumor data set to classify whether the case belongs to LGG or GBM:

Subtypes	1.5T (N)	3T (N)
LGG	51	48
GBM	256	138

Then, a harmonization module is trained to harmonize the 1.5T cases to the 3T cases.

The effectiveness is assessed by comparing the performance of the classifier on with/without harmonized test datasets.

Performance of computational modules before and after harmonisation

	AUC	Accuracy
Without harmonisation	0.621	0.723
Harmonised	0.671	0.857

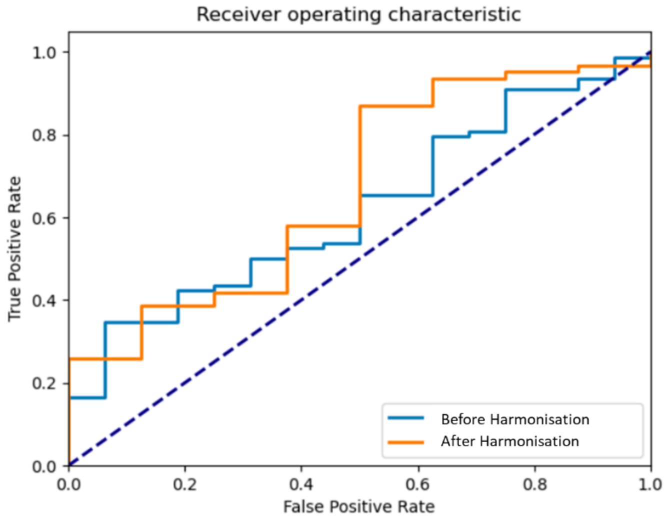

Automatic segmentation

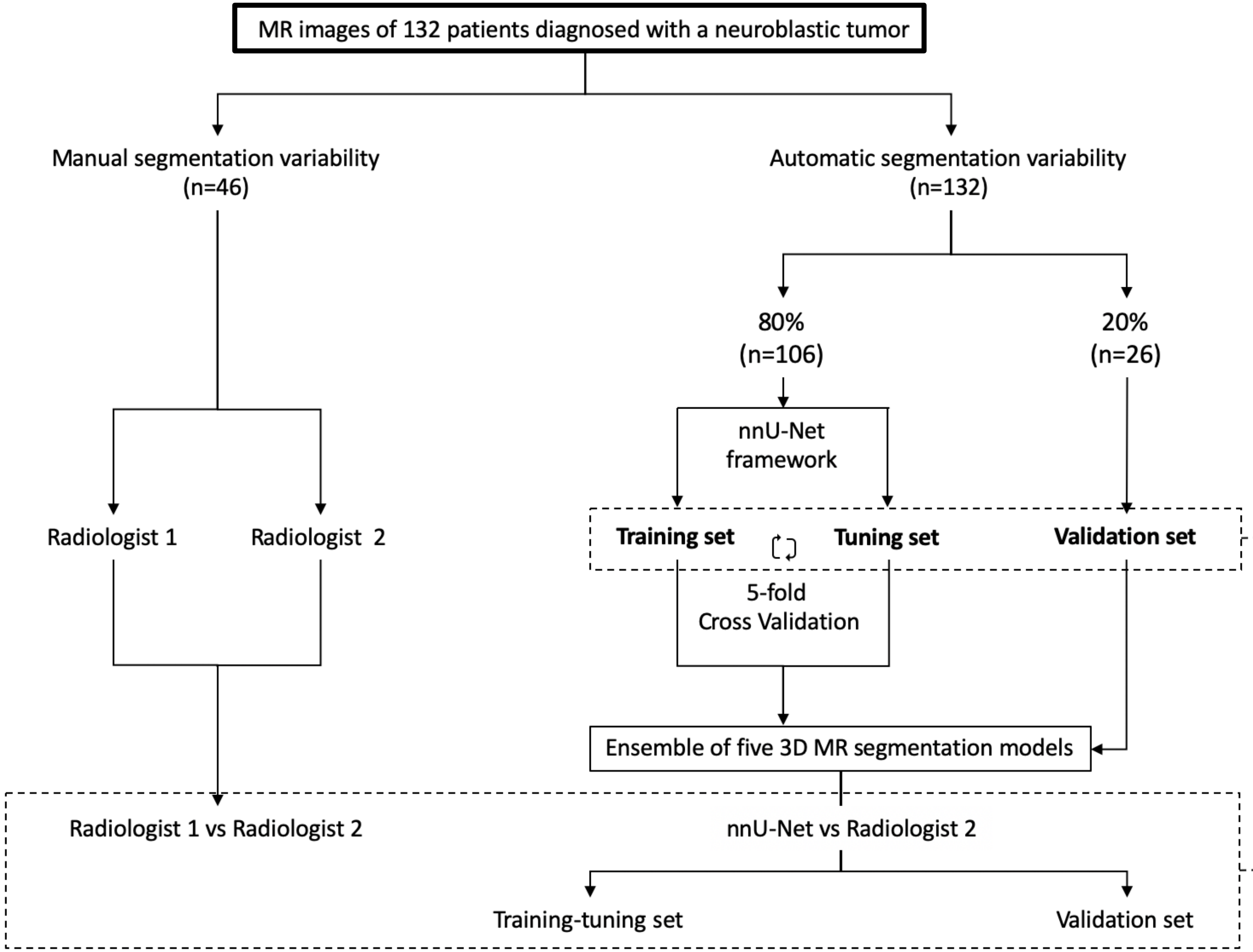

Balanced stratification
- Vendor
- Magnetic field strength
- Location
- Segmented sequence

Performance metrics
- DSC
- AUC ROC
- FPR
- FNR
- Time leverage

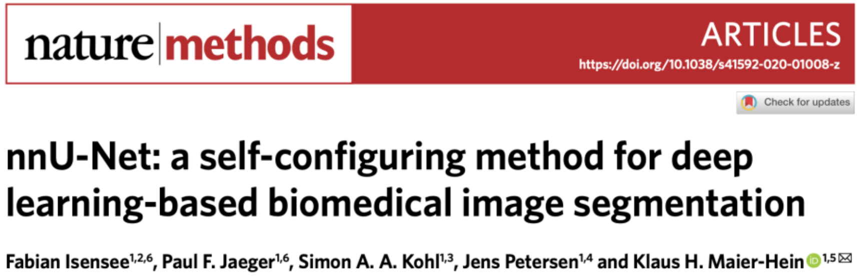
nature methods ARTICLES
https://doi.org/10.1038/s41592-020-01008-z
Check for updates

nnU-Net: a self-configuring method for deep learning-based biomedical image segmentation

Fabian Isensee[1,2,6], Paul F. Jaeger[1,6], Simon A. A. Kohl[1,3], Jens Petersen[1,4] and Klaus H. Maier-Hein[1,5]

Automatic vs manual segmentation variability

Inter-observer manual segmentation variability (n=46)

	DSC	AUC ROC
Median	**0.969**	0.998
IQR	0.032	0.004
Mean	0.934	0.983
SD	0.146	0.075

Automatic segmentation variability (n=106)

	DSC	AUC ROC
Median	**0.965**	0.981
IQR	0.018	0.010
Mean	0.931	0.964
SD	0.137	0.082

MR images segmentation variability of neuroblastic tumors is observed to be compatible between radiologists and the state-of-the-art deep learning architecture nnU-Net.

ACIM
HUP La Fe

Directional metrics

$$FPR = \frac{FP}{TP + FN}$$

$$FNR = \frac{FN}{TP + FN} = 1 - \text{Sensitivity or Recall}$$

Radiologist 1 manual segmentation
or
Automatic segmentation
(FP + TP)

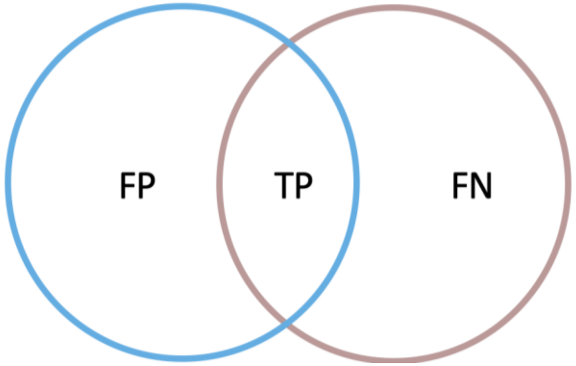

Radiologist 2 manual segmentation
"Ground truth"
(TP + FN)

Inter-observer manual segmentation variability (n=46)

	1-FPR	1-FNR
Median	**0.939**	0.998
IQR	0.063	0.008
Mean	0.895	0.968
SD	0.154	0.149

Automatic segmentation variability (n=106)

	1-FPR	1-FNR
Median	**0.968**	0.963
IQR	0.015	0.021
Mean	0.943	0.929
SD	0.132	0.164

The automatic segmentation model achieves a better performance regarding the FPR: great advantage for the posterior extraction of quantitative imaging features.

Visualization of results

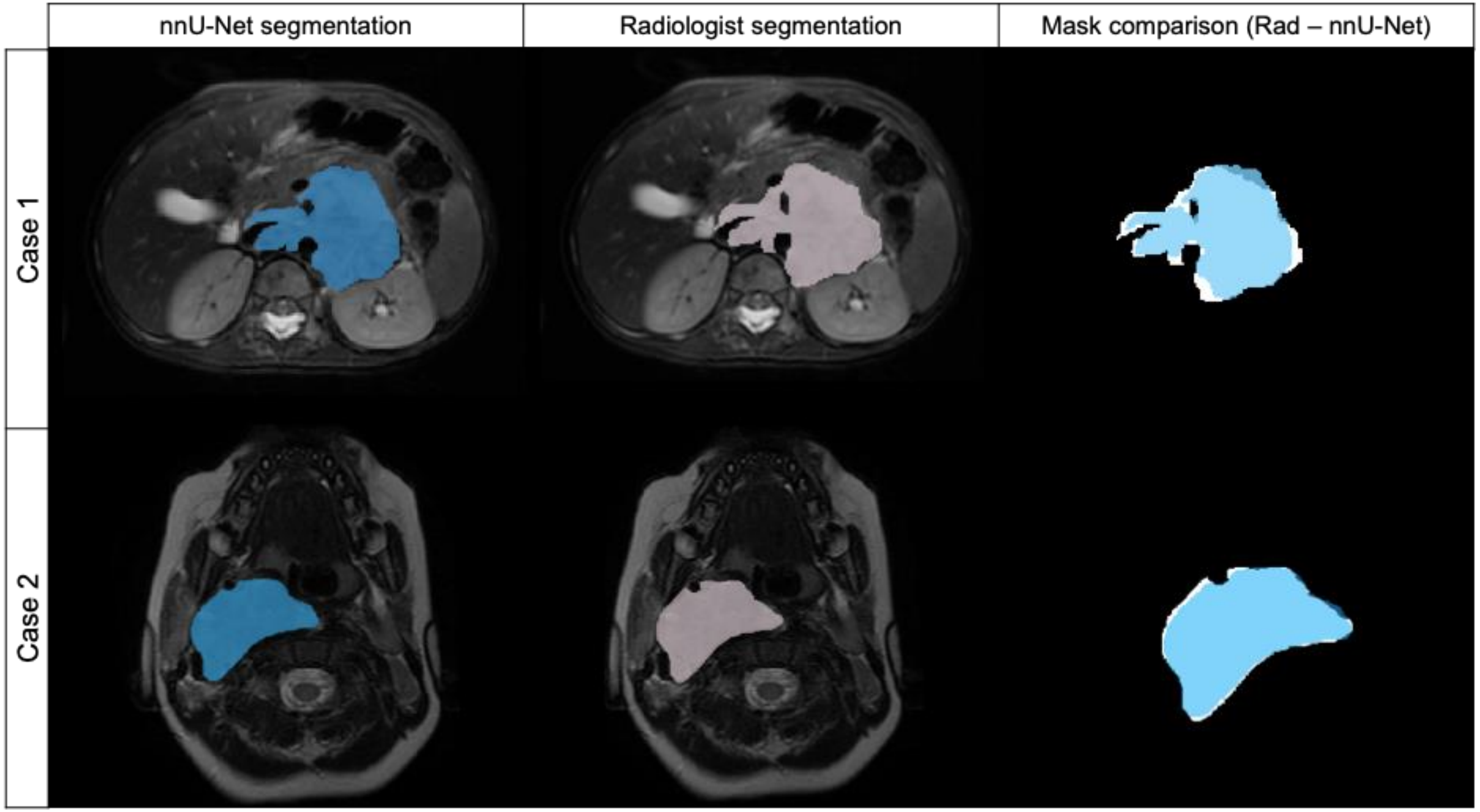

Radiomics

Radiomic features extraction (from T2-w image)

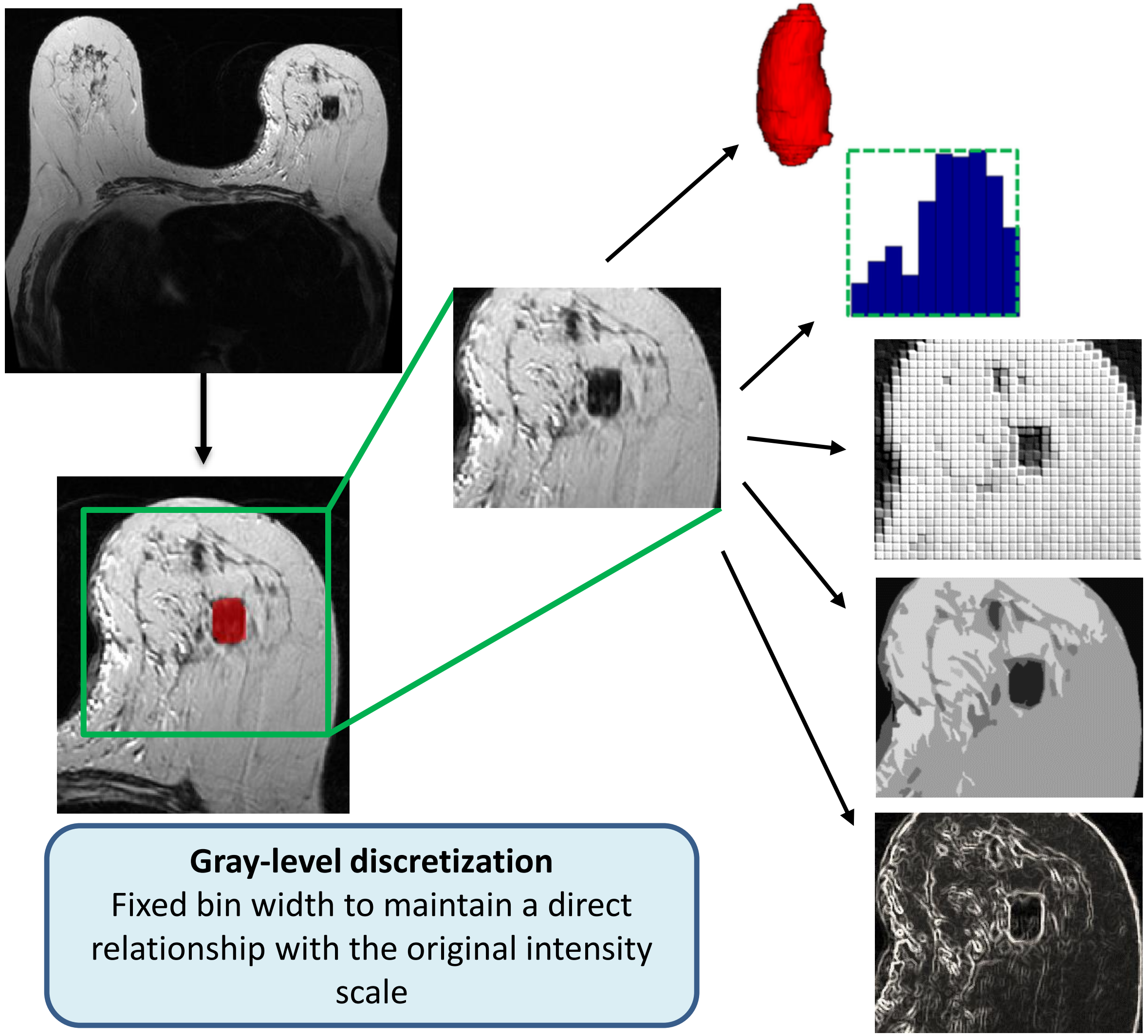

Shape
- Volume
- Elongation
- Sphericity
- Surface area
- Surface-Volume Ratio
- Flatness

Intensity
- Minimum
- Maximum
- Mean
- Variance
- Kurtosis
- Median
- SD
- RMS
- Skewness
- Energy
- Entropy
- Uniformity

Gray Level Cooccurence Matrix (GLCM)
- Joint energy
- Contrast
- Joint entropy
- Homogeneity
- Correlation
- Autocorrelation
- Sum average
- Sum variance
- Maximum probability
- Inverse variance
- Difference entropy
- Cluster Prominence

Gray Level Run Length Matrix (GLRLM)
- Small area emphasis
- Large area emphasis
- Gray level non-uniformity
- Size zone non-uniformity
- Zone percentage
- Gray level variance
- Zone variance
- Zone entropy
- Low / High gray level zone emphasis

Gray Level Size Zone Matrix (GLSZM)
- Short run emphasis
- Long run emphasis
- Gray level non-uniformity
- Run length non-uniformity
- Run percentage
- Run entropy
- Run variance
- Low gray level run emphasis
- High gray level run emphasis

Deep Features

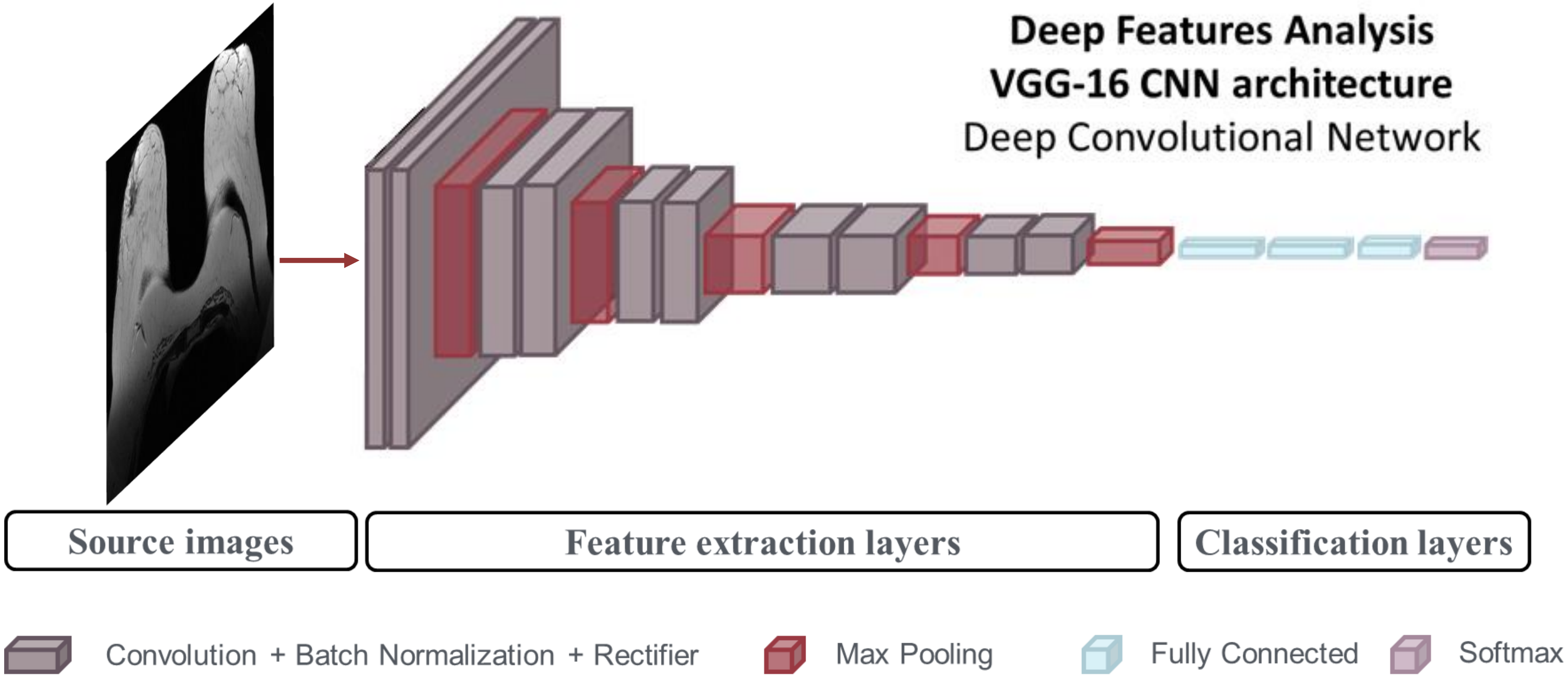

Feature extraction and “end-to-end” Neural Networks

Automation of the virtual biopsy process

- AI data generation: quantitative data related to relevant clinical outcomes.
- Segmentation, quantification and automatic and simultaneous prediction of final clinical endpoints with end-to-end AI methods.
- Integration of -omics data into the automated flow for decision making

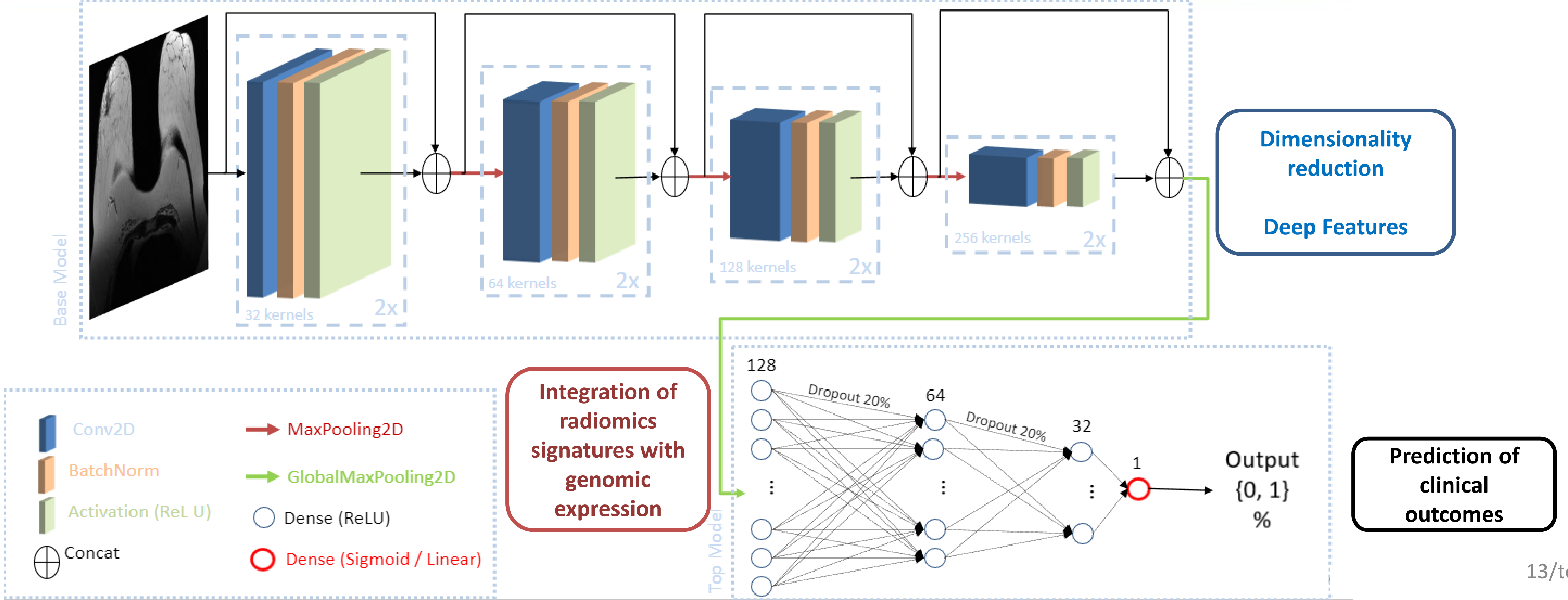

GIBI2[30] GRUPO DE INVESTIGACIÓN BIOMÉDICA EN IMAGEN

ACIM
HUP La Fe

Radiomic signatures

Low variance filter

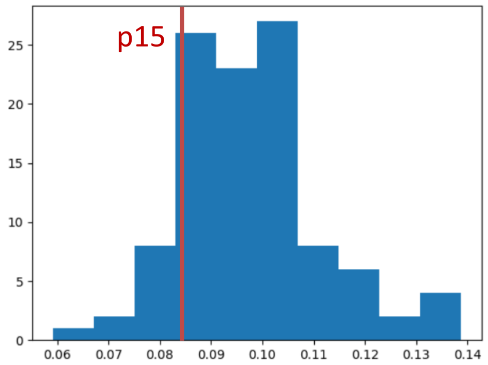

Data normalization

Study of dataset variances

Selecting the cutting threshold

Pearson's correlation matrix

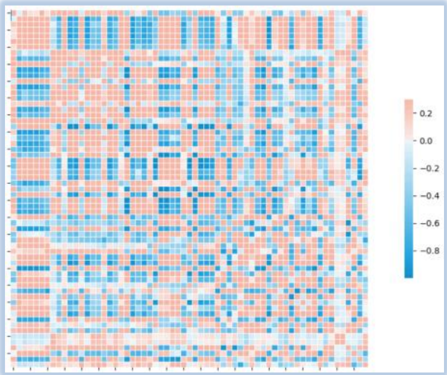

Selection of most correlated pair of features

Factor analysis: Varimax rotation

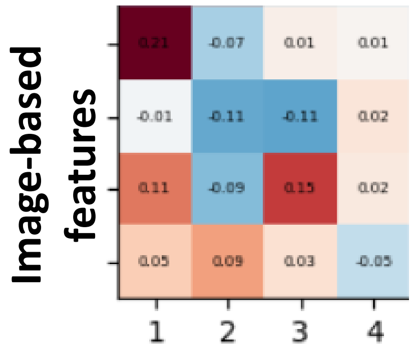

The rotation maximizes squared variances of weights

Simultaneous reduction of redundancies and dimensionality

GIBI2 30
GRUPO DE INVESTIGACIÓN BIOMÉDICA EN IMAGEN

ACIM
HUP La Fe

Outcomes prediction

1 Image-based signature

	0	1	2	3	4	5	6	7	8
original_glszm_ZoneVariance	0,3168773	0,1107472	0,0047431	0,0785443	0,0544485	0,0033883	0,032935	0,0336947	0,0021655
original_glszm_ZoneEntropy	0,2841487	0,0748367	0,1066504	0,041949	0,0120424	0,034301	0,0129585	0,0448946	0,0155192
original_ngtdm_Coarseness	0,251275	0,0763736	0,0358225	0,0673503	0,0098992	0,0068309	0,0047079	0,0731629	0,0097211
original_glszm_SmallAreaLowGrayLevelEmphasis	0,1776158	0,1954106	0,0298203	0,0763656	0,0477685	0,0026891	0,0235421	0,0047143	0,0120149
original_gldm_SmallDependenceEmphasis	0,0608665	0,2613982	0,0066042	0,0861982	0,030651	0,0024319	0,038865	0,0271704	0,0054516
original_gldm_LargeDependenceLowGrayLevelEmphasis	0,0417111	0,1860703	0,0276523	0,0507579	0,0542926	0,0301993	0,0398511	0,03571	0,0813643
original_glszm_HighGrayLevelZoneEmphasis	0,029904	0,2030425	0,0736933	0,0458689	0,0350695	0,0418297	0,0109821	0,0470235	0,0235679
original_gldm_DependenceNonUniformityNormalized	0,0273201	0,1591627	0,1287543	0,120316	0,0488221	0,0102605	0,0102596	0,0077138	0,0538781
original_firstorder_90Percentile	0,013751	0,2325216	0,020326	0,047377	0,0485453	0,0016606	0,0332317	0,0335815	0,0801144
original_firstorder_10Percentile	0,0124423	0,1323581	0,0797566	0,1211414	0,0633804	0,0003395	0,0489732	0,0081444	0,0868927
original_glcm_Imc1	0,0838359	0,1366301	0,1908377	0,0101026	0,0348266	0,0118145	0,0424073	0,0404133	0,0453294
original_glszm_SmallAreaEmphasis	0,0811051	0,1334598	0,1951023	0,0476971	0,0788423	0,0128489	0,0245588	0,0308119	0,0488153
original_glcm_Imc2	0,0780991	0,0069744	0,3051391	0,0071675	8,964E-05	0,0080682	0,0166093	0,0186514	0,0161352
original_glszm_GrayLevelNonUniformityNormalized	0,0717462	0,1271152	0,1899693	0,0047437	0,0394485	0,0007662	0,0362324	0,0245583	0,040289
original_glrlm_LongRunHighGrayLevelEmphasis	0,0488823	0,0856949	0,148322	0,0699018	0,0165139	0,0962726	0,016844	0,0230143	0,0285499
original_firstorder_Skewness	0,0481609	0,0291653	0,2108941	0,0330763	0,109092	0,0532184	0,0122485	0,0255769	0,0173831
original_gldm_SmallDependenceLowGrayLevelEmphasis	0,1376032	0,0284354	0,0388136	0,21191	0,0445079	0,0551639	0,0037854	0,0561831	0,065789
original_firstorder_TotalEnergy	0,1352088	0,0992226	0,0456963	0,1571289	0,0079631	0,0157465	0,0514724	0,0557969	0,0399127
original_gldm_LargeDependenceHighGrayLevelEmphasis	0,0629767	0,0322075	0,0158326	0,1905385	0,0640253	0,04166	0,0079303	0,0215461	0,0204211
original_shape_Elongation	0,054952	0,0216313	0,0313968	0,2275495	0,0117821	0,0708921	0,030483	0,038749	0,000697
original_shape_SurfaceVolumeRatio	0,0489144	0,0140705	0,0274847	0,2755079	0,0823871	0,0517045	0,0251206	0,0247302	0,0111615
original_shape_Flatness	0,0360608	0,0300132	0,002459	0,2094805	0,0075494	0,0150138	0,1082775	0,0171949	0,0350852
original_ngtdm_Strength	0,1273555	0,0014146	0,11941	0,0278437	0,2078517	0,0342684	0,0093461	0,0682568	0,0245715
original_firstorder_Kurtosis	0,034321	0,0488138	0,0159132	0,0477636	0,2721334	0,0136178	0,0023561	0,0264075	0,0081658
original_firstorder_Range	0,0115631	0,1069591	0,137758	0,0077579	0,192793	0,0131431	0,0165648	0,0881134	0,0152001
Kurtosis	0,0266759	0,0157758	0,0186937	0,023053	0,0212067	0,3208505	0,0117228	0,0093292	0,0234382
Std	0,0449643	0,0631879	0,0134729	0,0094275	0,0156489	0,0293623	0,2376475	0,0106654	0,0230907
original_glszm_SizeZoneNonUniformity	0,0812644	0,1281397	0,0833117	0,0474429	0,0431094	0,0324309	0,012616	0,2089814	0,0032956
original_firstorder_Minimum	0,040878	0,0086259	0,0581108	0,0440437	0,0403021	0,0906878	0,0363119	0,0018024	0,2117415

2 Image-based patient clustering

K-means algorithm (number of clusters= 2)

Cluster	0	1
Firstorder-Range-Value	114.762251	207.450179
GLCM-Jointentropy-Value	5.680005	7.600065
GLCM-Sumentropy-Value	4.002428	5.063923
Firstorder-Entropy-Value	3.250240	4.237091
Firstorder-Uniformity-Value	0.137684	0.067072
GLRLM-Graylevelnonuniformitynormalized-Value	0.123142	0.063780
NGTDM-Complexity-Value	262.359190	1444.623507
GLSZM-Highgraylevelzoneemphasis-Value	136.368705	332.483093
Firstorder-Maximum-Value	108.030538	195.627710
GLSZM-Graylevelnonuniformitynormalized-Value	0.081017	0.046500

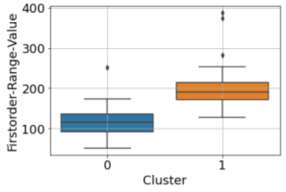

3 Overall survival

Kaplan-Meier Curve (Survival Analysis)

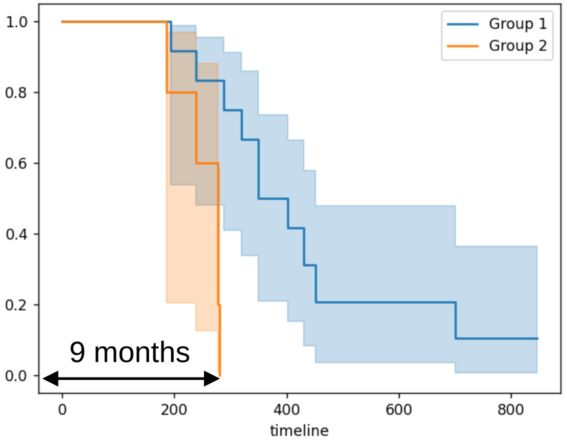

Conclusions

- Image-based signatures combined with data-driven unsupervised learning techniques can be a potential methodology for the classification of DIPG patients in terms of their overall survival.

Mean (days)	IQR (days)
252	40
415	86

Visual analysis of outcome predictions

Key Aspects

- Model to model comparison
- Confidence of each models predictions and its **relevant features**

Visualization

- Patient to Patient / Cohort comparison
- Comparative view of real/predicted outcomes
  1. Density distribution of clinical endpoints with its corresponding probability error (per bin)
  2. Feature Explainability (Shap value)
  3. Linked glyph preview feature distribution

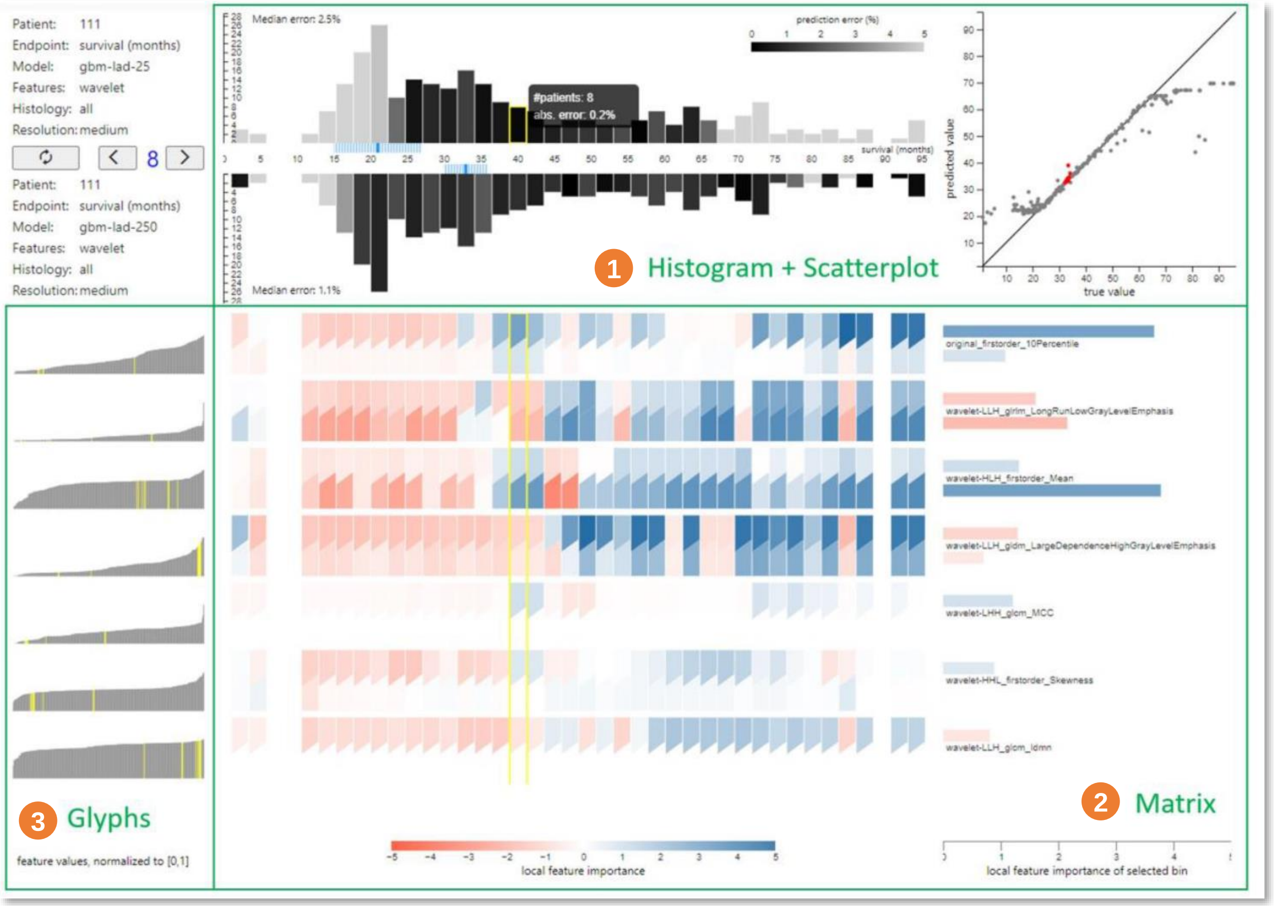

AI explicability and interpretability

Analysis per neuron

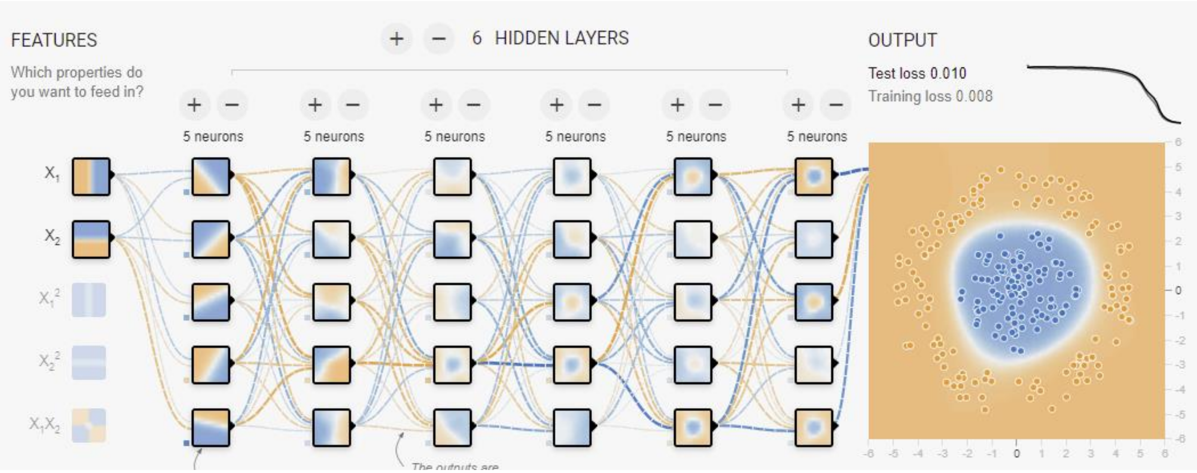

Gradient-weighted Class Activation Mapping (Grad-CAM)

Original image

Grad-CAM

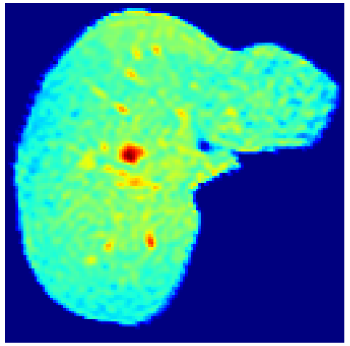

Overlay mapping

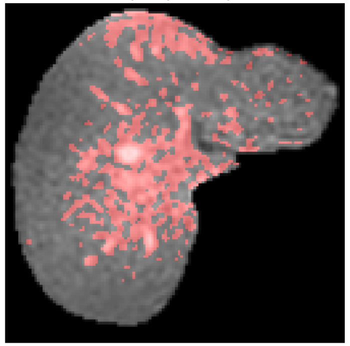

Neural Network → Convolutional Neural Network

ACIM
HUP La Fe

Implementation in clinical practice

- Adoption of AI solutions in routine clinical practice
- Continuous and Iterative Learning
- Lifetime adaptive monitoring in the real world
- Improved accuracy in treatment decision

Human-In-The-Loop (HITL)

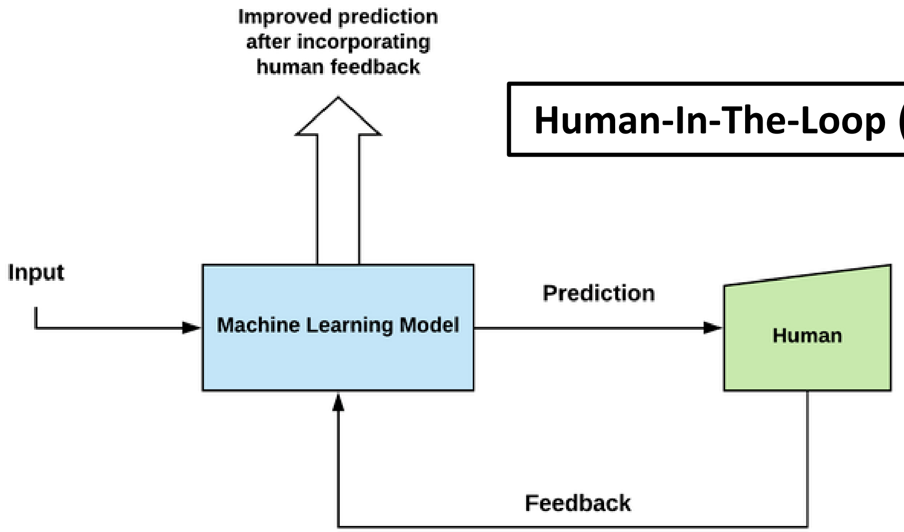

FUTURE-AI GUIDING PRINCIPLES

Fairness	For unbiased	ARTIFICIAL INTELLIGENCE SOLUTIONS IN MEDICAL IMAGING
Universality	For standardised	
Traceability	For monitoring	
Usability	For transferable	
Robustness	For reliable	
Explanability	For interpretable	

https://future-ai.eu/

ACIM
HUP La Fe

THANK YOU

Prof. Dr. Luis Martí Bonmatí

Biomedical Imaging Research Group (La Fe Health Research Institute)

Leonor Cerdá Alberich | leonor_cerda@iislafe.es